

Re-parameterized Low-rank Prompt: Generalize a Vision-Language Model within 0.5K Parameters

Tianxiang Hao^{1,2} Mengyao Lyu^{1,2} Hui Chen² Sicheng Zhao² Jungong Han³ Guiguang Ding^{1,2}
¹School of Software, Tsinghua University ²BNRist ³Computer Science Department, University of Sheffield
 {beyondhtx, jichenhui2012, jungonghan77}@gmail.com mengyao.lyu@outlook.com
 {schzhao, dinggg}@tsinghua.edu.cn

Abstract

With the development of large pre-trained vision-language models, how to effectively transfer the knowledge of such foundational models to downstream tasks becomes a hot topic, especially in a data-deficient scenario. Recently, prompt tuning has become a popular solution. When adapting the vision-language models, researchers freeze the parameters in the backbone and only design and tune the prompts. On the one hand, the delicate design of prompt tuning exhibits strong performance. On the other hand, complicated structures and update rules largely increase the computation and storage cost. Motivated by the observation that the evolution pattern of the generalization capability in visual-language models aligns harmoniously with the trend of rank variations in the prompt matrix during adaptation, we design a new type of prompt, Re-parameterized Low-rank Prompt (RLP), for both efficient and effective adaptation. Our method could largely reduce the number of tunable parameters and storage space, which is quite beneficial in resource-limited scenarios. Extensive experiments further demonstrate the superiority of RLP. In particular, RLP shows comparable or even stronger performance than the latest state-of-the-art methods with an extremely small number of parameters. On a series of tasks over 11 datasets, RLP significantly increases the average downstream accuracy of classic prompt tuning by up to 5.25% using merely 0.5K parameters.

1. Introduction

In recent years, vision-languages models [17, 37] have achieved tremendous success. Representative models like CLIP [37] are first pre-trained on a huge number of text-image pairs on the web to align textual and visual features, and then can be tuned and used for various downstream tasks.

However, traditional fine-tuning is not a good choice

to adapt vision-language models. Simply fine-tuning all the parameters can easily cause the model to forget task-agnostic knowledge that is general and important, and the huge training and storage cost is also an intractable problem. Prompt engineering, a recent popular method in natural language processing and computer vision, provides an overwhelming solution for the adaptation of vision-language models. Prompts are virtual tokens that are manually appended or prepended to the semantic tokens. Such virtual tokens can be hand-crafted designed and frozen [41], and they can be soft and tunable as well [18, 27, 30] for better transferability on different tasks. Typical prompt tuning methods freeze all the other parameters in the model and merely tune the prompts during adaptation.

In the vision-language field, prompt-based methods show good performance as well. CLIP [37] uses a hand-crafted text template for better zero-shot learning. Bahng *et al.* [1] adopts prompt tuning merely on the image encoder, CoOp [54] uses tunable text prompts to replace the fixed template in CLIP, CoCoOp [55] utilizes image feature to instruct the optimization of the soft text prompt in CoOp. [21, 24] simultaneously optimize image and text prompts and establish extra connections between isolated modalities. [3, 22, 47, 53] integrate strong regularization modules or losses into prompt tuning to diminish the overfitting and catastrophic forgetting problem. On the one hand, such delicate designs of prompt tuning in recent methods exhibits strong performance. On the other hand, their complicated structures and update rules largely increase the computation and storage cost.

Motivated by the observation that the evolution pattern of the generalization capability in visual-language models aligns harmoniously with the trend of rank variations in the prompt matrix during adaptation as shown in Fig. 2 and Tab. 1, we propose Re-parameterized Low-rank Prompt (RLP) to reach effective and efficient adaptation for vision-language models. For more details about the motivation and our observation, please refer to Sec. 2 and we will provide a thorough analysis. In this paper, we have explored how

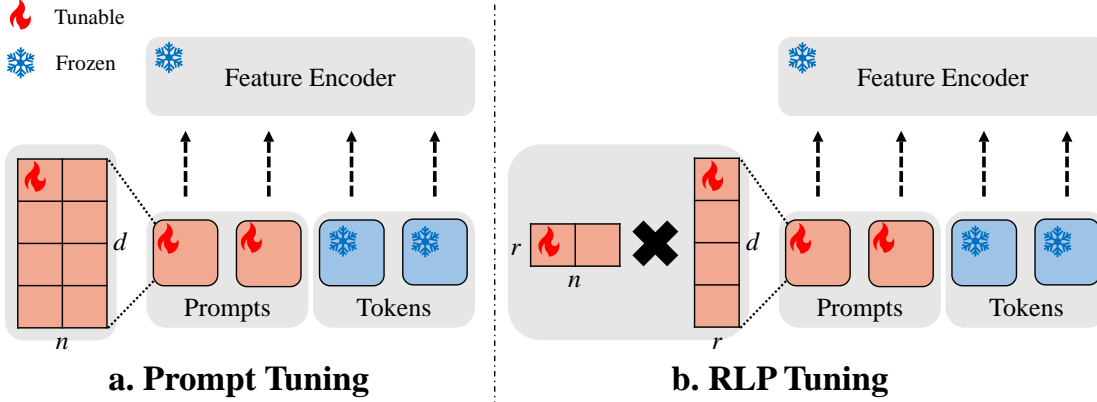


Figure 1. Comparison between classic prompt tuning and Re-parameterized Low-rank Prompt (RLP) tuning. RLP introduces two little parameter matrices in shape $[n, r]$ and $[r, d]$ separately, and uses the product of them as an equivalent low-rank prompt in shape $[n, d]$.

to effectively adapt vision-language models under an extremely small number of parameters. By choosing a small rank r , we could exceedingly compress the parameters used in adaptation. To the best of our knowledge, we are the first to reach comparable or even better performance compared with the latest state-of-the-art tuning methods in the base-to-new generalization and domain generalization using such barely few parameters, *i.e.* 0.5K.

Additionally, though more complex and delicate, existing methods are still refined on a common fundamental basis, *i.e.* prompt tuning. Such a common basis guarantees that our RLP could be easily and smoothly integrated into most of the off-the-shelf methods besides individually applied.

In summary, we conclude our contributions as follows:

- Motivated by the observation that the evolution pattern of the generalization capability in visual-language models aligns harmoniously with the trend of rank variations in the prompt matrix during adaptation, we propose to re-parameterize classic prompts into low-rank prompts for better accuracy and efficiency.
- We propose a novel initialization method and integrate Dropout layer as a lightweight regularization module to further improve the performance of low-rank prompt tuning without introducing any extra parameters and inference cost.
- We are the first to explore how to effectively adapt vision-language models using an extremely small number of parameters, *i.e.* 0.5K.
- We conduct extensive experiments and show the fantastic effectiveness and efficiency of our proposed method. In base-to-new generalization, domain generalization, cross-dataset transfer and few-shot learning settings, RLP consistently gives very competitive results, surpassing many state-of-the-art tuning methods though we use fewer parameters.

2. Motivation for Low-Rank Prompts

In this section, we provide the motivation for our design of low-rank prompts. First of all, we do classic prompt tuning on a CLIP [37] model following CoOp [54] and save checkpoint for every epoch. The prompts are randomly initialized here for clear observation. Since we want to inspect the rank properties of the prompt matrix, we do singular value decomposition (SVD) for the prompt matrix $P \in \mathbb{R}^{n \times d}$.

$$P = U\Sigma V^T \quad (1)$$

where Σ is the singular matrix and the values on its main diagonal denoted by σ_i ($1 \leq i \leq m$) are singular values, which are non-negative. Here $m = \min(n, d)$. The number of non-zero singular values is exactly the rank of the prompt matrix. In practice, even though all of the singular values are non-zero, the original matrix could be approximately considered a low-rank matrix as well if some singular values are far smaller than others. Therefore, we compute two values, “std” and “scale”, to investigate the low-rank property of singular values in training time. At a certain point during training, we denote the largest singular value as σ_{max} while the smallest singular value as σ_{min} . Since the SVD result is not unique, we do a scaling transformation first and then compute the standard deviation of the singular values.

$$\forall 1 \leq i \leq m, \sigma'_i = \frac{\sigma_i}{\sigma_{min}} \quad (2)$$

$$\text{std} = \sqrt{\frac{1}{m} \sum_{i=1}^m (\sigma'_i - \frac{\sum_{j=1}^m \sigma'_j}{m})^2} \quad (3)$$

We define “scale” as the ratio of the largest singular value and smallest singular value.

$$\text{scale} = \frac{\sigma_{max}}{\sigma_{min}} \quad (4)$$

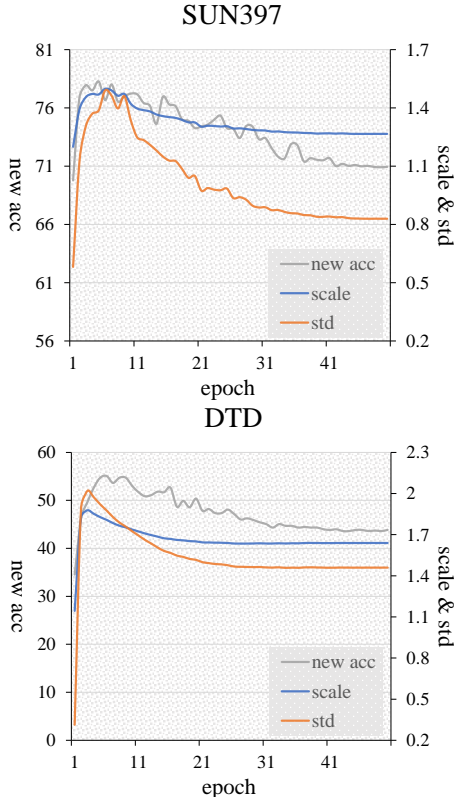


Figure 2. Curves for the generalization ability (represented by “new acc” here) and the singular value distribution of prompt matrix. When “new acc” increases, “std” and “scale” also increase, *i.e.* the prompt matrix is getting closer to a low-rank form.

Table 1. Spearman correlation coefficients. Clearly, accuracy in the new classes is strongly correlated with std/scale of the singular values of the prompt matrix.

	SUN397		DTD	
	std	scale	std	scale
new acc	0.967	0.970	0.907	0.782

Naturally, when the “std” is getting larger, the prompt matrix is getting closer to a low-rank form. The same holds true for the “scale”.

We show the result of each training epoch on base-to-new generalization setting in Fig. 2. The training curves are on two datasets, SUN397 [46] and DTD [4], respectively. Here we only show the test accuracy in the unseen new classes, which could measure the generalization ability of the model. For better visualization, we entirely scale up “std” to 8x and 6x on SUN397 and DTD respectively to match the value of “scale”, so we could put them under the same axis in the figure. We also compute the Spearman correlation coefficient in Tab. 1, which measures the statistical dependence between the rankings of two variables. Seen from Fig. 2 and Tab. 1, the generalization ability of the vision-language model is highly correlated with “std” and

“scale”, *e.g.* the Spearman correlation coefficient of “std” and “new acc” is 0.967 on SUN397.

In summary, during training, the adaptation ability of the model represented by accuracy on the base classes is consistently improved as we have demonstrated in ???. The generalization ability of the model is improved in the first few epochs as well. However, as the training goes on, the generalization ability starts dropping, which indicates that the model suffers from overfitting and catastrophic forgetting problems. Seen from Fig. 2, the fluctuation trend of “new acc” is highly consistent with “std” and “scale”. Naturally, we can infer that the low-rank form of the prompt matrix is beneficial to the generalization ability of the vision-language models. Motivated by such observation and inference, we propose Re-parameterized Low-rank Prompts (RLP) to get better generalization ability. Moreover, low-rank prompts naturally contain fewer parameters compared with classic ones, and thus we can also earn efficiency improvements.

3. Related Works

3.1. Vision-Language Models

Recently, large-scale vision-language models have shown very competitive performance in various tasks. Classic works [17, 37, 48, 49, 51] learn the multi-modal representation by a self-supervised manner on a large amount of image-text pairs. The representative work CLIP [37] is a milestone, which aligns the vision representation and language representation by contrastive learning and shows excellent performance. A well-trained vision-language model is a great treasure, which could largely facilitate the development of various related fields. There have been successful applications of such strong models on few-shot recognition [54, 55], detection [9, 32, 39, 50] and segmentation [6, 26, 31, 38]. For video data, there are also works on video classification [36] and video understanding [20].

3.2. Prompt Tuning

Originating from natural language processing, prompts are first introduced as a fixed template [41], *e.g.* *a photo of a* ..., which is hand-crafted and fixed. Later, a series of methods [19, 25, 27–29, 42] are proposed to make such prompts tunable and be optimized during adaptation. Prompt tuning could adaptively narrow the gap between pre-trained representations and downstream tasks, significantly facilitating the fine-tuning process. Representative prompt tuning methods would add tunable virtual tokens, *i.e.* prompts, along with the semantic tokens as inputs of the model. All of the tokens are processed together to get text embeddings first and then sent to the feature encoder. Witnessing the success of prompting language models, researchers design prompts [18, 52] for visual models in a similar way. In

vision-language field, there are several explorations as well. Bahng *et al.* [1] adopts prompt tuning merely on the image encoder. CoOp [54] uses tunable text prompts to replace the fixed template in CLIP [37]. CoCoOp [55] utilizes image feature to instruct the optimization of the tunable text prompts in CoOp. [21, 24] simultaneously optimize image and text prompts and establish extra connections between different modals. [3, 22, 47, 53] integrate strong regularization modules or losses into prompt tuning to diminish the overfitting and catastrophic forgetting problem. For better downstream accuracy, researchers design more and more complicated methods, accompanied by inefficiency. To solve the problem, we propose Re-parameterized Low-rank Prompt (RLP) to take the place of classic prompts, which can largely decrease the number of tunable parameters and further enhance the model’s generalization ability. Notice that though becoming more complex, existing methods are still refined on a common fundamental basis, *i.e.* prompt tuning. Such a common basis guarantees that RLP could be easily and smoothly integrated into most of the off-the-shelf methods besides individually applied.

4. Methodology

4.1. A Review of Prompt Tuning for CLIP

In this subsection, we first make a brief review of CLIP [37] which is used as our foundational model. CLIP consists of a text encoder \mathcal{L} and an image encoder \mathcal{V} . Typically, \mathcal{L} is a language transformer, while \mathcal{V} can be a convolutional neural network or a vision transformer. In this paper, we follows [54, 55] to use a ViT-B/16 [7] as the image encoder \mathcal{V} unless specifically mentioned. We will make a review of how to prompt a CLIP for downstream image recognition in the following paragraphs.

Text Encoder Suppose there are M layers in the text encoder. For k -th layer \mathcal{L}_k , the inputs are a series of prompt tokens P_{k-1}^l and a $[CLS]$ token c_{k-1}^l , and the outputs are P_k^l and c_k^l . The inputs of the first layer P_0^l and c_0^l are exactly the word embeddings of the prompts along with the label, *e.g.* “A photo of a $[CLS]$ ” or just some randomly initialized vectors. Formally, we have $P_k^l \in \mathbb{R}^{n^l \times d^l}$ and $c_k^l \in \mathbb{R}^{d^l}$, where n^l denotes the text prompts’ length and d^l denotes the dimension of word embedding. $\forall 1 \leq k \leq M$, we have

$$[P_k^l, c_k^l] = \mathcal{L}_k([P_{k-1}^l, c_{k-1}^l]) \quad (5)$$

The output feature of the text encoder $f^l \in \mathbb{R}^{d^v}$, where d^v is the dimension of the visual feature space, is generated by projecting the $[CLS]$ token of the last layer to the visual space by a linear transformation, *i.e.* $f^l = \text{Proj}(c_M^l)$.

Image Encoder Suppose there are N layers in the image encoder. For k -th layer \mathcal{V}_k , the inputs are a series of image patch tokens I_{k-1} , a classification token c_{k-1}^v and prompt

tokens P_{k-1}^v , and the outputs are I_k , c_k^v and P_k^v . The inputs of the first layer I_0 and c_0^v are exactly the patch embeddings of the input image and the pre-trained class token. P_0^v is randomly initialized in general. Formally, we have $I_k \in \mathbb{R}^{p \times d^v}$, $c_k^v \in \mathbb{R}^{d^v}$ and $P_k^v \in \mathbb{R}^{n^v \times d^v}$, where p denotes the number of image patches and d^v denotes the dimension of visual embedding. $\forall 1 \leq k \leq N$, we have

$$[P_k^v, c_k^v, I_k] = \mathcal{V}_k([P_{k-1}^v, c_{k-1}^v, I_{k-1}]) \quad (6)$$

The output feature of the image encoder is $f^v = c_N^v$.

Prediction CLIP can be easily used for image classification. Suppose there are C classes, and $\{f_c^l\}_{c=1}^C$ are the corresponding text features. The probability of label y is

$$p(y|f^v) = \frac{\exp(\text{sim}(f^v, f_y^l)/\tau)}{\sum_{c=1}^C \exp(\text{sim}(f^v, f_c^l)/\tau)} \quad (7)$$

where $\text{sim}(\cdot, \cdot)$ denotes cosine similarity function and τ is temperature. The final prediction is $\hat{z} = \arg \max_{1 \leq y \leq C} (p(y|f^v))$.

It is worth noting that some researchers adopt a deeper manner [18, 21] to organize the prompts. They directly add and tune the prompt in each layer in the feature encoder, instead of inheriting the output prompt calculated by the last encoder, *i.e.* a forward pass becomes

$$[-, c_k^l] = \mathcal{L}_k([P_{k-1}^l, c_{k-1}^l]) \quad (8)$$

and

$$[-, c_k^v, I_k] = \mathcal{V}_k([P_{k-1}^v, c_{k-1}^v, I_{k-1}]) \quad (9)$$

Each P^l/P^v contains tunable parameters.

4.2. Re-parameterized Low-rank Prompts

4.2.1 Low-rank Decomposition

Motivated by the observation in Sec. 2, we re-parameterize the origin full-rank prompt matrix into a low-rank form in adaptation for better generalizability and efficiency.

Formally, given a typical text or image prompt matrix $P \in \mathbb{R}^{n \times d}$, we take inspiration from LoRA [16] to create two low-dimensional matrices and use their product as the final low-rank prompt. Suppose the intrinsic rank is r , then we first randomly initialize $P_A \in \mathbb{R}^{n \times r}$ and $P_B \in \mathbb{R}^{r \times d}$. The low-rank prompt P_{lr} is

$$P_{lr} = P_A P_B \quad (10)$$

Here P_{lr} is in the same shape with normal full rank prompt P . As a result, we could do a low-rank prompt tuning by sending P_{lr} rather than the original P into the corresponding feature encoder as shown in Eqs. (5) and (6), and updating the parameters in P_A and P_B through the back-propagated gradients.

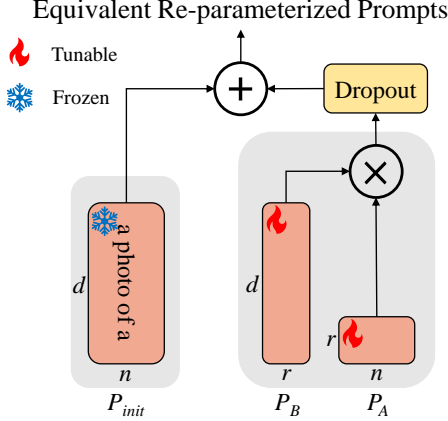


Figure 3. To take full advantage of some special initialization form of prompts, e.g. a hand-crafted template *a photo of a* for the text prompts, we introduce a concurrent full-rank prompt branch along with the proposed low-rank prompts. By turning off the gradient of the newly added branch, we start training from a promising initial point, and the total number of tunable parameters or stored parameters will not increase as well. The Dropout layer could effectively regularize the update of low-rank prompts and alleviate overfitting and catastrophic forgetting. Better still, Dropout is a lightweight non-parametric layer and turns out to be an Identity layer in inference, resulting in negligible cost.

4.2.2 Full-rank Initialization

In the field of tuning vision-language models, existing works have confirmed that the initialization method of prompts is quite important. For example, [54, 55] adopt a hand-crafted template as the initial point of the text prompts, and [24] copies the parameters in the text or image class token to initialize the prompts of the corresponding branch. If we just do a random initialization, the overall performance of such existing methods would drop severely. See Sec. 5.2 for more details. In other words, it would be helpful if we could take advantage of a good initial point.

The problem lies in the fact that artificially designed initialization P_{init} is almost certain to be full rank, i.e. $\text{rank}(P_{init}) = \min(n, d)$, and our current low-rank prompt $P_{lr} = P_A P_B$ could only express the matrices whose rank is less or equal than r . Since $r < \min(n, d)$, it is impossible to directly initialize P_A and P_B by a given P_{init} .

To solve such a problem, we add a concurrent branch of full-rank prompts $P_{fr} \in \mathbb{R}^{n \times d}$ along with the proposed low-rank prompts as shown in Fig. 3. Naturally, $P_{fr} = P_{init}$. And we randomly sample P_A/P_B from a Gaussian distribution in which $\mu = 0$ and $\sigma \rightarrow 0$. A small σ here could avoid constant initialization and enrich the update paths. Notably, P_{fr} is kept frozen during the whole adaptation, and thus it would not increase the number of tunable or stored parameters.

4.2.3 Regularization

As discussed in Sec. 3, existing works have shown that proper regularization would significantly improve the generalization ability. Therefore, to alleviate overfitting and catastrophic forgetting, we put a Dropout layer with drop ratio p after the low-rank branch as displayed in Fig. 3.

Therefore, the input prompt of the feature encoder is

$$P = P_{fr} + \text{Dropout}(P_{lr}, p) \quad (11)$$

Finally, we have

$$P = P_{init} + \text{Dropout}(P_A P_B, p) \quad (12)$$

4.3. Efficiency Analysis

The whole adaptation process of a pre-trained vision-language model can be divided into three parts: training, storage and inference. In this subsection, we will analyze the efficiency of CLP in each part separately.

Training In the training phase, the number of tunable parameters in total is $r(n + d)$. Compared with classic prompt tuning which has nd tunable parameters, we can largely reduce the trainable parameters by choosing a small r satisfying $r \ll \min(n, d)$. Such reduction could help us train the model faster and use less memory during training than those delicate-designed methods with massive complicated structures and update rules.

Storage After training, we just store P_A and P_B onto the disk for every downstream task. Similar to the training period, the number of stored parameters is $r(n + d)$. In contrast, classic prompt tuning stores a much larger set of nd parameters. As a result, we can save a fairly large amount of storage space when there are lots of tasks to be adapted.

Inference Before inference, we first load P_{init} , P_A and P_B from disk to memory. Noticing that Dropout is exactly an identity layer in the inference mode, we could pre-calculate the equivalent P by

$$P = P_{init} + P_A P_B \quad (13)$$

and just keep P in the memory. For inference, we directly use P as the input prompts, and thus the inference cost is the same as classic prompt tuning. Some existing methods add complex bridges between the isolated parameters to earn extra improvements, e.g. CoCoOp [55]. There ain't no such thing as a free lunch. They would face slower speed and huge memory occupation in inference time.

4.4. Advantages of RLP

- **Efficiency and Effectiveness** To our knowledge, we are the first one to reach comparable or even better performance with state-of-the-art methods using a fairly small number of parameters, i.e. 516. RLP reaches an excellent trade-off between efficiency and effectiveness.

- **Simplicity** Replacing the classic prompt by RLP just needs to modify several lines of code. The design of RLP merely changes the structure of prompts. No special loss nor extra module is introduced.
- **Robustness** RLP is relatively capable of anti-disturbance. As in Tab. 3, RLP could maximally reserve its knowledge from domain shift.
- **Plug and Play** In a classic transformer model, RLP only affects its prompts, which are very basic and necessary components in modern transformer-based architectures. Such characteristic enables us to plug RLP into most of the existing prompt tuning methods by simply replacing several lines of code.

5. Experiments

To verify the effectiveness of the proposed method, we evaluate our method and make comparisons with the latest state-of-the-art methods in terms of the following problems:

1. **Base-to-new generalization**, which models are trained with base classes and evaluated on both base and new classes.
2. **Domain generalization**, which aims to show generalization to the domain shift, especially for out-of-distribution data.
3. **Cross-dataset transfer**, which aims to see if the method has the potential to transfer beyond a single dataset. It is a much more challenging problem because the fundamentals can be totally changed across different datasets.
4. **Few-shot learning**, which aims to evaluate the adaptation performance of the model to extract knowledge from a dataset whose samples are very few, *e.g.* 1, 2, 4, 8 or 16 samples.

All methods, including the baseline methods, in our experiments, are initialized with the same CLIP weights provided by the open-source CLIP [37]¹. In order to give details about the experimental setup, we first introduce the used datasets, the compared baseline methods, and the implementation details.

Datasets Following previous work [54, 55], we leverage 11 image recognition datasets to verify the effectiveness of the proposed method for both the base-to-new generalization task. These datasets include two datasets for the generic object classification, *i.e.*, ImageNet [5] and Caltech101 [8], five datasets for the fine-grained classification, *i.e.*, OxfordPets [35], StanfordCars [23], Flowers102 [34], Food101 [2] and FGVC Aircraft [33], one dataset for the scene recognition, *i.e.*, SUN397 [46], one dataset for the action recognition, *i.e.*, UCF101 [43], one dataset for the texture classification, *i.e.*, DTD [4], and one dataset for the satellite image recognition, *i.e.*, EuroSAT [12].

For the domain generalization task, we utilize ImageNet-A [14], ImageNet-R [13], ImageNetv2 [40] and ImageNet-S [44] to verify the robustness of the model. In this setting, we need to first train the model using ImageNet, and then directly use images from other four datasets to do inference.

For the cross-dataset transfer task, the datasets are the same as those of the base-to-new generalization task. Similar to domain generalization, the model will be first trained on ImageNet and then do inference on the other 10 different datasets.

For the few-shot learning task, the datasets are the same as those of the base-to-new generalization task. The model will be trained and evaluated with 1, 2, 4, 8 and 16 shots separately.

The dataset splitting is exactly the same as previous works [54, 55]. We report the averaged model performance over three runs with different random seeds for fair comparisons.

Competitors

1. **CLIP** [37] (ICML 2021): CLIP is a strong baseline vision-language model that is pre-trained on a large number of image-text pairs from the web by learning a contrastive objective. CLIP enables strong zero-shot adaptation ability on various downstream tasks by using fixed text prompts, *i.e.* *a photo of a*.
2. **CoOp** [54] (IJCV 2022): CoOp replaces the fixed text prompts in CLIP with tunable text prompts to improve the adaptation ability of the vision-language model. CoOp shows excellent performance in few-shot situations.
3. **CoCoOp** [55] (CVPR 2022): CoCoOp replaces the isolated tunable text prompts in CoOp with conditional text prompts, which receive extra gradients from the image features besides text features. CoCoOp largely improves the generalization ability of the vision-language model, getting good results on base-to-new generalization and domain adaptation.
4. **CLIP-Adapter** [10] (arxiv): CLIP-Adapter adopts the thoughts of classic Adapter [15] to use serial linear layers and activation functions to adapt for downstream tasks. It is simple yet effective in few-shot learning.
5. **ProGrad** [56] (ICCV 2023): ProGrad only updates the text and image prompts whose gradient are aligned (or non-conflicting) to the general knowledge, which is represented as the optimization direction offered by the pre-defined prompt predictions. Such regularization helps it finish good adaptation and generalization.

Training Details Following previous work [55], we employ ViT-B/16 as the image encoder in the CLIP. Each training image is resized to 224×224 before being fed into the image encoder. Some common data augmentation strategies, *e.g.*, random crop and random flip, are used to enhance

¹<https://github.com/openai/CLIP>.

Table 2. Comparisons with latest methods in base-to-new generalization. H: harmonic mean [45]. Overall, RLP shows the strongest performance compared with other latest tuning methods. RLP reaches highest average harmonic mean accuracy and wins on 7 of 11 datasets with far more fewer parameters.

(a) Average over 11 datasets.				(b) ImageNet.			(c) Caltech101.					
#params	Base	New	H	Base	New	H	Base	New	H			
CLIP	0K	69.34	74.22	71.70	CLIP	72.43	68.14	70.22	CLIP	96.84	94.00	95.40
CoOp	2.1K	82.69	63.22	71.66	CoOp	76.47	67.88	71.92	CoOp	98.00	89.81	93.73
CoCoOp	35.4K	80.47	71.69	75.83	CoCoOp	75.98	70.43	73.10	CoCoOp	97.96	93.81	95.84
Adapter	525.5K	82.62	70.97	76.35	Adapter	76.53	66.67	71.26	Adapter	98.20	93.20	95.63
ProGrad	8.2K	82.79	68.55	75.00	ProGrad	77.03	68.80	72.68	ProGrad	98.50	91.90	95.09
RLP	0.5K	79.86	74.17	76.91	RLP	76.07	70.87	73.37	RLP	97.90	95.03	96.45

(d) OxfordPets.				(e) StanfordCars.			(f) Flowers102.				
Base	New	H		Base	New	H	Base	New	H		
CLIP	91.17	97.26	94.12	CLIP	63.37	74.89	68.65	CLIP	72.08	77.80	74.83
CoOp	93.67	95.29	94.47	CoOp	78.12	60.40	68.13	CoOp	97.60	59.67	74.06
CoCoOp	95.20	97.69	96.43	CoCoOp	70.49	73.59	72.01	CoCoOp	94.87	71.75	81.71
Adapter	94.40	94.10	94.25	Adapter	77.13	69.23	72.97	Adapter	97.70	70.83	82.13
ProGrad	94.40	95.10	94.75	ProGrad	79.00	67.93	73.05	ProGrad	96.27	71.07	81.77
RLP	95.17	97.77	96.45	RLP	70.00	75.10	72.46	RLP	94.80	74.97	83.72

(g) Food101.				(h) FGVC Aircraft.			(i) SUN397.				
Base	New	H		Base	New	H	Base	New	H		
CLIP	90.10	91.22	90.66	CLIP	27.19	36.29	31.09	CLIP	69.36	75.35	72.23
CoOp	88.33	82.26	85.19	CoOp	40.44	22.30	28.75	CoOp	80.60	65.89	72.51
CoCoOp	90.70	91.29	90.99	CoCoOp	33.41	23.71	27.74	CoCoOp	79.74	76.86	78.27
Adapter	90.40	90.40	90.40	Adapter	39.57	32.27	35.55	Adapter	81.67	73.93	77.61
ProGrad	90.17	89.53	89.85	ProGrad	42.63	26.97	33.04	ProGrad	80.70	71.03	75.56
RLP	90.73	91.83	91.28	RLP	35.17	35.57	35.37	RLP	79.47	77.70	78.57

(j) DTD.				(k) EuroSAT.			(l) UCF101.				
Base	New	H		Base	New	H	Base	New	H		
CLIP	53.24	59.90	56.37	CLIP	56.48	64.05	60.03	CLIP	70.53	77.50	73.85
CoOp	79.44	41.18	54.24	CoOp	92.19	54.74	68.69	CoOp	84.69	56.05	67.46
CoCoOp	77.01	56.00	64.85	CoCoOp	87.49	60.04	71.21	CoCoOp	82.33	73.45	77.64
Adapter	80.47	52.23	63.35	Adapter	86.93	64.20	73.86	Adapter	85.80	73.63	79.25
ProGrad	76.70	46.67	58.03	ProGrad	91.37	56.53	69.85	ProGrad	83.90	68.50	75.42
RLP	74.27	60.33	66.58	RLP	81.57	61.67	70.23	RLP	83.33	75.03	78.97

Table 3. Comparisons with latest methods in domain generalization. RLP gets comparable or even better results with the latest state-of-the-art methods with much fewer parameters, showing excellent robustness for domain shift.

#params	Source ImageNet	Target				Average	
		-V2	-Sketch	-Adversarial	-Rendition		
CLIP	0K	66.73	60.83	46.15	47.77	73.96	57.18
CoOp	2.1K	71.51	64.20	47.99	49.71	75.21	59.28
CoCoOp	35.4K	71.02	64.07	48.75	50.63	76.18	59.91
Adapter	525.5K	69.33	62.53	47.67	49.17	75.42	58.70
ProGrad	8.2K	72.24	64.73	47.61	49.39	74.58	59.07
RLP	0.5K	70.80	63.95	49.07	50.97	77.19	60.30

the model performance, following [55]. During training, we set the batch size as 32. We employ the stochastic gradient

descent algorithm (SGD) to optimize the learnable parameters. As [54], we utilize a warm-up scheme at the first

Table 4. Results in the cross-dataset transfer setting. RLP gives the highest accuracy on 6 of 10 datasets, and slightly outperforms CoCoOp by a small margin on average though the source accuracy of RLP is a bit lower. Such result well demonstrates that RLP could maximally extract general and data-agnostic knowledge from given images.

	# params	Source	Target										Average
		ImageNet	Caltech101	Pets	Cars	Flowers	Food101	Aircraft	Sun397	DTD	EuroSAT	UCF101	
CoOp	2.1K	71.51	93.70	89.14	64.51	68.71	85.30	18.47	64.15	41.92	46.39	66.55	63.88
CoCoOp	35.4K	71.02	94.43	90.14	65.32	71.88	86.06	22.94	67.36	45.73	45.37	68.21	65.74
Adapter	525.5K	69.33	93.43	88.87	64.40	70.27	85.63	24.67	65.80	44.90	47.70	66.00	65.17
RLP	0.5K	70.57	94.20	90.50	67.17	71.27	86.07	23.83	67.60	46.73	42.10	68.93	65.84

epoch, which is important for the tuning of prompts. For all the other baselines, we strictly follow the configurations of their original papers.

For RLP, we conduct a grid search to find the optimal hyper-parameters based on the configuration of CoOp. We chose CoOp, the most lightweight prompt-tuning method, as well as the weakest method as our foundational model. In Sec. 5.1, we set the rank $r = 1$ in RLP for all the settings in Sec. 5.1. The total number of tunable parameters in RLP is $4 * 1 + 1 * 512 = 516$, which is merely around 0.25x of that in CoOp. In Sec. 5.2, we will show how to turn such a weak baseline CoOp into an effective and efficient method step by step, only with the support of such 516 parameters.

5.1. Main Results

5.1.1 Base-to-new Generalization

Following previous works [54, 55], for each dataset, we split its classes equally into two non-overlapping groups, *i.e.*, one as base classes and the other as new classes. We train all models on the base classes and perform a base/new evaluation on the base/new classes.

The results are shown in Tab. 2. Overall, RLP still shows the strongest performance, and the superiority mainly relies on the improvement of new classes. In other words, RLP largely improves the generalization ability of CLIP. In particular, compared with our direct baseline CoOp, RLP gets 10.95% accuracy gain on the new classes and 2.83% accuracy drop on the base classes. Such a result tells us that our low-rank prompt and lightweight regularization design reach our initial purpose to make the model more generalizable, instead of overfitting every upcoming dataset.

Notably, compared with the latest lightweight method ProGrad, even if RLP only uses <20x of its parameters, RLP still outperforms it by a clear margin, which clearly demonstrates the excellent effectiveness and efficiency of our proposed method.

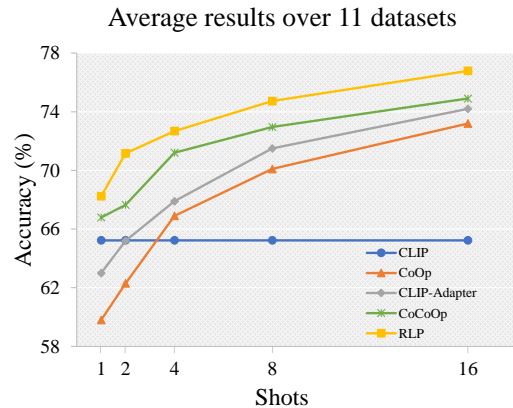


Figure 4. Average results of few-shot learning over 11 datasets.

5.1.2 Domain Generalization

Then we follow CoCoOp [55] to use ImageNet, ImageNet-A, ImageNet-R, ImageNet-v2, and ImageNet-S to run domain generalization experiments to verify the robustness of RLP. Results are shown in Tab. 3. As seen from the table, on target datasets, RLP gets comparable or even better average accuracy compared with the latest methods. Importantly, RLP uses much fewer parameters and thus can reach significantly better efficiency. For CLIP, CoOp, CLIP-Adapter and ProGrad, there is a clear performance gap between our RLP and them.

5.1.3 Cross-dataset Transfer

Finally, we follow CoCoOp [55] to conduct cross-dataset transfer evaluation. Results are shown in Tab. 4. We can see that on the source dataset, CoOp accomplishes the highest score, which is similar with the situation in the base-to-new generalization setting. However, concentrating too much on the current dataset will absolutely cause overfitting and catastrophic forgetting problems, and finally lead to a severe drop in the performance on those unseen datasets. In this setting, RLP wins on 6 of 10 datasets and its average accuracy is also slightly better than the best competitor Co-

Table 5. Ablation study on base-to-new generalization setting

	Low-rank prompts	Full-rank init	Dropout	#params	base	new	H
CoOp	-	-	-	2.1K	82.69	63.22	71.66
RLP	✓	-	-	0.5K	79.91	71.48	75.46
	✓	✓	-	0.5K	79.42	73.21	76.19
	✓	✓	✓	0.5K	79.70	73.59	76.53

Table 6. Training, storage, and inference efficiencies.

	#params	Training throughput	Inference throughput
CoOp	2.1K	93 image/s	738 images/s
CoCoOp	35.4K	5 images/s	13 images/s
ProGrad	8.2K	56 images/s	732 images/s
RLP	0.5K	91 images/s	738 images/s

CoOp. Such result well demonstrates that RLP could maximally extract general and data-agnostic knowledge from given images compared with other prompt-based methods. Considering the huge difference in the parameter numbers, we could summarize that RLP is still the better choice.

5.1.4 Few-shot Learning

In this paragraph, we will show the experiment results of RLP in the few-shot learning setting. This setting is originated from CoOp. Seen from Fig. 4, RLP consistently outperforms zero-shot CLIP, CoOp, and CLIP-Adapter across all the shot numbers. Such results demonstrate the superiority of RLP in adaptation ability when there are few samples in downstream tasks.

Overall, in base-to-new generalization, domain generalization, cross-dataset transfer and few-shot learning, the proposed method can consistently accomplish state-of-the-art performance while enjoying extremely high parameter efficiency, fruitfully demonstrating the effectiveness and efficiency of the proposed method.

5.2. Analysis

5.2.1 Ablation study

We first investigate the impact of each component in the proposed method RLP. We revise the baseline model, *i.e.*, CoOp [54] which adopts full-rank tunable text prompt, step-by-step.

Our modifications start with transforming the text encoder. We first replace the tunable prompt tokens with our low-rank prompt tokens, denoted as “Low-rank prompts”, for the CoOp method. After replacing the classic prompts with our low-rank prompts, the average Harmonic accuracy over 11 datasets directly improved from 71.66% to 75.46%. The accuracy on the base classes decreases by 2.78% and

on the new classes increases by 8.26%. Although the adaptation ability for base classes slightly drops, the generalization ability for new classes raises quite a lot. This phenomenon proves that our low-rank design is fairly beneficial for the model’s generalization ability once again.

Then we integrate the re-parameterized full-rank initialization into CoOp. The harmonic mean accuracy improves by 1.27%. Here we can see the importance of special initialization, even if we have already changed the prompt format from full-rank to low-rank.

Finally, we add a delicate selected lightweight regularization layer, Dropout, to the current module. Dropout helps us alleviate the overfitting problem, and avoid catastrophic forgetting. Therefore, we get a very competitive result, 76.53% Harmonic average accuracy, which is completely comparable to some latest lightweight state-of-the-art methods.

5.2.2 Efficiency Comparison

In this paragraph, we will give a comprehensive analysis of all the training, storage, and inference efficiencies for RLP and several existing methods. Since the parameter scale of CLIP-Adapter [10] is significantly larger than others, we do not contain CLIP-Adapter into comparison.

For a fair comparison, we do all the speed tests on the same GPU. Results are shown in Tab. 6. Our proposed RLP shares nearly the same fastest training and inference speeds with the simplest method CoOp, and more importantly, RLP merely uses 0.5K parameters, which is a lot more storage-efficient than other methods. Specially, compared with classic method CoCoOp, RLP enjoys **>18x** training speed, **>56x** inference speed and **<70x** storage usage. Besides complex structures, the huge gap in the inference speed is partly owing to the huge memory cost of CoCoOp, which forces us to adopt a smaller batch size than other methods for CoCoOp. Moreover, compared with the latest method ProGrad, RLP enjoys **>1.6x** training speed, comparable inference speed, and **<60x** storage usage, which adequately demonstrates the super efficiency of RLP.

5.2.3 Results for Convolutional Image Encoder

In this subsection, we will show the experiment results of RLP on CLIP with convolutional image encoder ResNet-50 [11], rather than the default ViT-B/16 [7]. Seen from

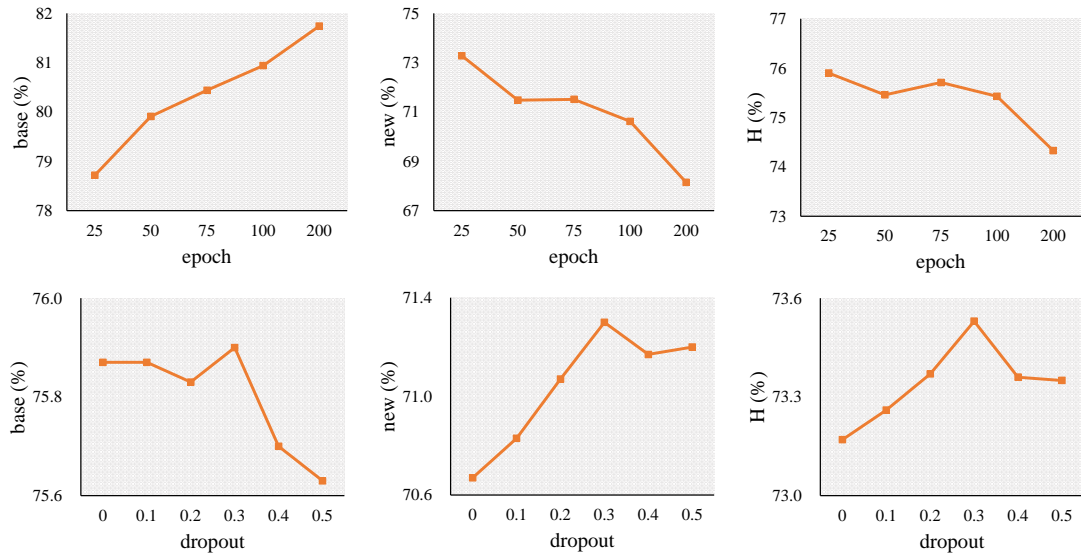


Figure 5. Top line: Results of different training epochs on base-to-new generalization. Bottom line: Results of different dropout ratios on base-to-new generalization.

Table 7. Average results on 11 datasets for CLIP with convolutional image encoder, ResNet-50 [11].

	image encoder	#params	base	new	H
CoOp	ResNet-50	2.1K	77.16	61.01	68.14
ProGrad	ResNet-50	8.2K	73.29	65.96	69.06
RLP	ResNet-50	0.5K	75.22	64.98	69.73

Table 8. Results of adding RLP to image prompts on ImageNet.

	#params	base	new	H
Text RLP	0.5K	75.87	70.67	73.17
Image RLP	0.5K	74.57	69.40	71.89

Tab. 7, compared with baseline CoOp, RLP still largely improves the new accuracy and the harmonic mean accuracy over 11 datasets, while the base accuracy slightly drops. Compared with the latest method ProGrad, RLP shows clear superiority on base accuracy and the harmonic mean accuracy.

5.2.4 Results for Using RLP on the Image Side

There are several works [18, 21] indicating the effectiveness of the image prompts. Therefore, in this subsection, we will explore the results of applying RLP to image prompts. Seen from Tab. 8, using RLP on the image side also reaches high accuracy. However, the base, new, and average accuracy of image RLP is not as good as those of text RLP. Such

experiment result tells us to use RLP on the text side instead of the image side when we aim to reach high accuracy with extremely few parameters.

5.2.5 Results across Different Hyper-parameters

Effect of Different Epochs In this paragraph, we investigate that how the total training epoch could influence the adaptation result. As shown in Fig. 5, we select a series of epoch numbers, *i.e.* 25, 50, 75, 100, and 200. And we run an experiment using RLP to get the corresponding results for the given epoch. We could see that as the training epoch increases, the accuracy on base classes continues decreasing while the accuracy on new classes continues increasing. It is reasonable because as the training continues, the model has a higher and higher risk of forgetting its original knowledge and overfitting the current dataset. To reach a better harmonic mean accuracy, a good trade-off is necessary.

Effect of Different Dropout Ratios In this paragraph, we will show the influence of different dropout ratios in RLP on ImageNet. Seen from Fig. 5, as the dropout ratio increases, the base accuracy starts decreasing while the new accuracy starts increasing in most cases. The harmonic mean accuracy first increases and then decreases. Such a result is reasonable. Since a high dropout ratio can be regarded as a kind of strong regularization, proper regularization will help avoid overfitting and catastrophic forgetting problems. However, too strong regularization will damage the ability of the model.

Table 9. Results of different ranks on ImageNet.

rank	#params	base	new	H
1	0.5K	75.87	70.67	73.17
2	1.0K	76.03	70.13	72.96
3	1.5K	76.20	70.40	73.19

Table 10. Results of different combinations of learning rates and weight decays under 16-shot learning setting on ImageNet

Acc \ wd	wd		
	1e-4	5e-4	1e-3
1e-3	70.73	70.67	70.78
2e-3	70.80	70.83	70.77
3e-3	70.83	70.83	70.81

Effect of Different Ranks In this paragraph, we will show the influence of different ranks in RLP. Seen from Tab. 9, roughly, a larger rank brings more parameters, higher base accuracy, and lower new accuracy. As a result, increasing rank is not necessarily able to improve the average accuracy.

Effect of Different Learning Rates and Weight Decays

In this paragraph, we investigate the effect of normal hyper-parameters learning rate and weight decay. We wonder if tuning them carefully would lead to significant improvement. Seen from Tab. 10, the performance of RLP stays stable whatever the learning rate and weight decay vary. The conclusion here is that our method RLP is robust for learning rate and weight decay.

6. Conclusion

With the development of huge vision-language models, how to effectively and efficiently adapt such huge models to various downstream tasks becomes a challenging problem. Much effort has been made to leverage the potential of prompt tuning in adapting vision-language models. However, existing methods usually suffer from inefficiency. To solve such a problem, we propose Re-parameterized Low-rank Prompts (RLP) for a better trade-off between effectiveness and efficiency in vision-language adaptation. Along with the low-rank prompt design, we further propose a novel initialization method and integrate the Dropout layer as a lightweight regularization module to further improve the performance without introducing any extra parameters and inference cost. We are the first to explore how to effectively adapt vision-language models using an extremely small number of parameters, *i.e.* 0.5K. Besides efficiency and effectiveness, RLP has many other advantages such as simplicity and robustness, which are quite valuable in real-world application scenarios. Extensive experiments show that even if RLP uses much fewer parameters, RLP could

still consistently be comparable to or better than state-of-the-art methods.

References

- [1] Hyojin Bahng, Ali Jahanian, Swami Sankaranarayanan, and Phillip Isola. Visual prompting: Modifying pixel space to adapt pre-trained models. *arXiv preprint arXiv:2203.17274*, 2022. 1, 4
- [2] Lukas Bossard, Matthieu Guillaumin, and Luc Van Gool. Food-101—mining discriminative components with random forests. In *ECCV*, 2014. 6
- [3] Adrian Bulat and Georgios Tzimiropoulos. Lasp: Text-to-text optimization for language-aware soft prompting of vision & language models. In *Proceedings of the IEEE/CVF Conference on Computer Vision and Pattern Recognition*, pages 23232–23241, 2023. 1, 4
- [4] Mircea Cimpoi, Subhransu Maji, Iasonas Kokkinos, Sammy Mohamed, and Andrea Vedaldi. Describing textures in the wild. In *CVPR*, 2014. 3, 6
- [5] Jia Deng, Wei Dong, Richard Socher, Li-Jia Li, Kai Li, and Li Fei-Fei. Imagenet: A large-scale hierarchical image database. In *CVPR*, 2009. 6
- [6] Jian Ding, Nan Xue, Gui-Song Xia, and Dengxin Dai. Decoupling zero-shot semantic segmentation. In *Proceedings of the IEEE/CVF Conference on Computer Vision and Pattern Recognition*, pages 11583–11592, 2022. 3
- [7] Alexey Dosovitskiy, Lucas Beyer, Alexander Kolesnikov, Dirk Weissenborn, Xiaohua Zhai, Thomas Unterthiner, Mostafa Dehghani, Matthias Minderer, Georg Heigold, Sylvain Gelly, et al. An image is worth 16x16 words: Transformers for image recognition at scale. In *International Conference on Learning Representations*, 2020. 4, 9
- [8] Li Fei-Fei, Rob Fergus, and Pietro Perona. Learning generative visual models from few training examples: An incremental bayesian approach tested on 101 object categories. In *CVPR-W*, 2004. 6
- [9] Chengjian Feng, Yujie Zhong, Zequn Jie, Xiangxiang Chu, Haibing Ren, Xiaolin Wei, Weidi Xie, and Lin Ma. Prompt-det: Towards open-vocabulary detection using uncurated images. In *European Conference on Computer Vision*, pages 701–717. Springer, 2022. 3
- [10] Peng Gao, Shijie Geng, Renrui Zhang, Teli Ma, Rongyao Fang, Yongfeng Zhang, Hongsheng Li, and Yu Qiao. Clip-adapter: Better vision-language models with feature adapters. *arXiv preprint arXiv:2110.04544*, 2021. 6, 9
- [11] Kaiming He, Xiangyu Zhang, Shaoqing Ren, and Jian Sun. Deep residual learning for image recognition. In *Proceedings of the IEEE conference on computer vision and pattern recognition*, pages 770–778, 2016. 9, 10
- [12] Patrick Helber, Benjamin Bischke, Andreas Dengel, and Damian Borth. Eurosat: A novel dataset and deep learning benchmark for land use and land cover classification. *IEEE Journal of Selected Topics in Applied Earth Observations and Remote Sensing*, 2019. 6
- [13] Dan Hendrycks, Steven Basart, Norman Mu, Saurav Kadavath, Frank Wang, Evan Dorundo, Rahul Desai, Tyler Zhu,

- Samyak Parajuli, Mike Guo, Dawn Song, Jacob Steinhardt, and Justin Gilmer. The many faces of robustness: A critical analysis of out-of-distribution generalization. *ICCV*, 2021. 6
- [14] Dan Hendrycks, Kevin Zhao, Steven Basart, Jacob Steinhardt, and Dawn Song. Natural adversarial examples. *CVPR*, 2021. 6
- [15] Neil Houlsby, Andrei Giurgiu, Stanislaw Jastrzebski, Bruna Morrone, Quentin De Laroussilhe, Andrea Gesmundo, Mona Attariyan, and Sylvain Gelly. Parameter-efficient transfer learning for nlp. In *International Conference on Machine Learning*, pages 2790–2799. PMLR, 2019. 6
- [16] Edward J Hu, Yelong Shen, Phillip Wallis, Zeyuan Allen-Zhu, Yuanzhi Li, Shean Wang, Lu Wang, and Weizhu Chen. Lora: Low-rank adaptation of large language models. *arXiv preprint arXiv:2106.09685*, 2021. 4
- [17] Chao Jia, Yinfei Yang, Ye Xia, Yi-Ting Chen, Zarana Parekh, Hieu Pham, Quoc Le, Yun-Hsuan Sung, Zhen Li, and Tom Duerig. Scaling up visual and vision-language representation learning with noisy text supervision. In *International Conference on Machine Learning*, pages 4904–4916. PMLR, 2021. 1, 3
- [18] Menglin Jia, Luming Tang, Bor-Chun Chen, Claire Cardie, Serge Belongie, Bharath Hariharan, and Ser-Nam Lim. Visual prompt tuning. *arXiv preprint arXiv:2203.12119*, 2022. 1, 3, 4, 10
- [19] Zhengbao Jiang, Jun Araki, Haibo Ding, and Graham Neubig. How can we know when language models know? on the calibration of language models for question answering. *Transactions of the Association for Computational Linguistics*, 9:962–977, 2021. 3
- [20] Chen Ju, Tengda Han, Kunhao Zheng, Ya Zhang, and Weidi Xie. Prompting visual-language models for efficient video understanding. In *European Conference on Computer Vision*, pages 105–124. Springer, 2022. 3
- [21] Muhammad Uzair Khattak, Hanoona Rasheed, Muhammad Maaz, Salman Khan, and Fahad Shahbaz Khan. Maple: Multi-modal prompt learning. In *Proceedings of the IEEE/CVF Conference on Computer Vision and Pattern Recognition*, pages 19113–19122, 2023. 1, 4, 10
- [22] Muhammad Uzair Khattak, Syed Talal Wasim, Muzammal Naseer, Salman Khan, Ming-Hsuan Yang, and Fahad Shahbaz Khan. Self-regulating prompts: Foundational model adaptation without forgetting. In *Proceedings of the IEEE/CVF International Conference on Computer Vision*, pages 15190–15200, 2023. 1, 4
- [23] Jonathan Krause, Michael Stark, Jia Deng, and Li Fei-Fei. 3d object representations for fine-grained categorization. In *ICCV-W*, 2013. 6
- [24] Dongjun Lee, Seokwon Song, Jihee Suh, Joonmyeong Choi, Sanghyeok Lee, and Hyunwoo J Kim. Read-only prompt optimization for vision-language few-shot learning. In *Proceedings of the IEEE/CVF International Conference on Computer Vision*, pages 1401–1411, 2023. 1, 4, 5
- [25] Brian Lester, Rami Al-Rfou, and Noah Constant. The power of scale for parameter-efficient prompt tuning. *arXiv preprint arXiv:2104.08691*, 2021. 3
- [26] Boyi Li, Kilian Q Weinberger, Serge Belongie, Vladlen Koltun, and Rene Ranftl. Language-driven semantic segmentation. In *International Conference on Learning Representations*, 2022. 3
- [27] Xiang Lisa Li and Percy Liang. Prefix-tuning: Optimizing continuous prompts for generation. *arXiv preprint arXiv:2101.00190*, 2021. 1, 3
- [28] Pengfei Liu, Weizhe Yuan, Jinlan Fu, Zhengbao Jiang, Hiroaki Hayashi, and Graham Neubig. Pre-train, prompt, and predict: A systematic survey of prompting methods in natural language processing. *arXiv preprint arXiv:2107.13586*, 2021.
- [29] Xiao Liu, Kaixuan Ji, Yicheng Fu, Zhengxiao Du, Zhilin Yang, and Jie Tang. P-tuning v2: Prompt tuning can be comparable to fine-tuning universally across scales and tasks. *arXiv preprint arXiv:2110.07602*, 2021. 3
- [30] Xiao Liu, Yanan Zheng, Zhengxiao Du, Ming Ding, Yujie Qian, Zhilin Yang, and Jie Tang. Gpt understands, too. *arXiv preprint arXiv:2103.10385*, 2021. 1
- [31] Timo Lüddecke and Alexander Ecker. Image segmentation using text and image prompts. In *Proceedings of the IEEE/CVF Conference on Computer Vision and Pattern Recognition*, pages 7086–7096, 2022. 3
- [32] Muhammad Maaz, Hanoona Rasheed, Salman Khan, Fahad Shahbaz Khan, Rao Muhammad Anwer, and Ming-Hsuan Yang. Class-agnostic object detection with multi-modal transformer. In *The European Conference on Computer Vision*. Springer, 2022. 3
- [33] Subhransu Maji, Esa Rahtu, Juho Kannala, Matthew Blaschko, and Andrea Vedaldi. Fine-grained visual classification of aircraft. *arXiv preprint arXiv:1306.5151*, 2013. 6
- [34] Maria-Elena Nilsback and Andrew Zisserman. Automated flower classification over a large number of classes. In *ICVGIP*, 2008. 6
- [35] Omkar M Parkhi, Andrea Vedaldi, Andrew Zisserman, and CV Jawahar. Cats and dogs. In *CVPR*, 2012. 6
- [36] Rui Qian, Yeqing Li, Zheng Xu, Ming-Hsuan Yang, Serge Belongie, and Yin Cui. Multimodal open-vocabulary video classification via pre-trained vision and language models. *arXiv preprint arXiv:2207.07646*, 2022. 3
- [37] Alec Radford, Jong Wook Kim, Chris Hallacy, Aditya Ramesh, Gabriel Goh, Sandhini Agarwal, Girish Sastry, Amanda Askell, Pamela Mishkin, Jack Clark, et al. Learning transferable visual models from natural language supervision. In *International Conference on Machine Learning*, pages 8748–8763. PMLR, 2021. 1, 2, 3, 4, 6
- [38] Yongming Rao, Wenliang Zhao, Guangyi Chen, Yansong Tang, Zheng Zhu, Guan Huang, Jie Zhou, and Jiwen Lu. Denseclip: Language-guided dense prediction with context-aware prompting. In *Proceedings of the IEEE/CVF Conference on Computer Vision and Pattern Recognition*, pages 18082–18091, 2022. 3
- [39] Hanoona Abdul Rasheed, Muhammad Maaz, Muhammad Uzair Khattak, Salman Khan, and Fahad Khan. Bridging the gap between object and image-level representations for open-vocabulary detection. In *Advances in Neural Information Processing Systems*, 2022. 3

- [40] Benjamin Recht, Rebecca Roelofs, Ludwig Schmidt, and Vaishal Shankar. Do imagenet classifiers generalize to imagenet? In *International conference on machine learning*, pages 5389–5400. PMLR, 2019. 6
- [41] Timo Schick and Hinrich Schütze. Exploiting cloze questions for few shot text classification and natural language inference. *arXiv preprint arXiv:2001.07676*, 2020. 1, 3
- [42] Taylor Shin, Yasaman Razeghi, Robert L Logan IV, Eric Wallace, and Sameer Singh. Autoprompt: Eliciting knowledge from language models with automatically generated prompts. In *Proceedings of the 2020 Conference on Empirical Methods in Natural Language Processing (EMNLP)*, pages 4222–4235, 2020. 3
- [43] Khurram Soomro, Amir Roshan Zamir, and Mubarak Shah. Ucf101: A dataset of 101 human actions classes from videos in the wild. *arXiv preprint arXiv:1212.0402*, 2012. 6
- [44] Haohan Wang, Songwei Ge, Zachary Lipton, and Eric P Xing. Learning robust global representations by penalizing local predictive power. In *Advances in Neural Information Processing Systems*, pages 10506–10518, 2019. 6
- [45] Yongqin Xian, Bernt Schiele, and Zeynep Akata. Zero-shot learning-the good, the bad and the ugly. In *CVPR*, 2017. 7
- [46] Jianxiong Xiao, James Hays, Krista A Ehinger, Aude Oliva, and Antonio Torralba. Sun database: Large-scale scene recognition from abbey to zoo. In *CVPR*, 2010. 3, 6
- [47] Hantao Yao, Rui Zhang, and Changsheng Xu. Visual-language prompt tuning with knowledge-guided context optimization. In *Proceedings of the IEEE/CVF Conference on Computer Vision and Pattern Recognition*, pages 6757–6767, 2023. 1, 4
- [48] Lewei Yao, Runhui Huang, Lu Hou, Guansong Lu, Minzhe Niu, Hang Xu, Xiaodan Liang, Zhenguo Li, Xin Jiang, and Chunjing Xu. FILIP: Fine-grained interactive language-image pre-training. In *International Conference on Learning Representations*, 2022. 3
- [49] Lu Yuan, Dongdong Chen, Yi-Ling Chen, Noel Codella, Xiyang Dai, Jianfeng Gao, Houdong Hu, Xuedong Huang, Boxin Li, Chunyuan Li, et al. Florence: A new foundation model for computer vision. *arXiv preprint arXiv:2111.11432*, 2021. 3
- [50] Yuhang Zang, Wei Li, Kaiyang Zhou, Chen Huang, and Chen Change Loy. Open-vocabulary detr with conditional matching. *arXiv preprint arXiv:2203.11876*, 2022. 3
- [51] Xiaohua Zhai, Xiao Wang, Basil Mustafa, Andreas Steiner, Daniel Keysers, Alexander Kolesnikov, and Lucas Beyer. Lit: Zero-shot transfer with locked-image text tuning. In *Proceedings of the IEEE/CVF Conference on Computer Vision and Pattern Recognition*, pages 18123–18133, 2022. 3
- [52] Yuanhan Zhang, Kaiyang Zhou, and Ziwei Liu. Neural prompt search. *arXiv preprint arXiv:2206.04673*, 2022. 3
- [53] Kecheng Zheng, Wei Wu, Ruili Feng, Kai Zhu, Jiawei Liu, Deli Zhao, Zheng-Jun Zha, Wei Chen, and Yujun Shen. Regularized mask tuning: Uncovering hidden knowledge in pre-trained vision-language models. In *Proceedings of the IEEE/CVF International Conference on Computer Vision*, pages 11663–11673, 2023. 1, 4
- [54] Kaiyang Zhou, Jingkang Yang, Chen Change Loy, and Ziwei Liu. Learning to prompt for vision-language models. *International Journal of Computer Vision*, 130(9):2337–2348, 2022. 1, 2, 3, 4, 5, 6, 7, 8, 9
- [55] Kaiyang Zhou, Jingkang Yang, Chen Change Loy, and Ziwei Liu. Conditional prompt learning for vision-language models. In *Proceedings of the IEEE/CVF Conference on Computer Vision and Pattern Recognition*, pages 16816–16825, 2022. 1, 3, 4, 5, 6, 7, 8
- [56] Beier Zhu, Yulei Niu, Yucheng Han, Yue Wu, and Hanwang Zhang. Prompt-aligned gradient for prompt tuning. In *Proceedings of the IEEE/CVF International Conference on Computer Vision*, pages 15659–15669, 2023. 6